

An Experimental and Analytical study of Fatigue Crack Shape Control by Cold Working

F. P. Brennan¹, S. S. Ngiam² and C. W. Lee³

¹School of Engineering, Whittle Building, Cranfield University, Cranfield, Beds, MK43 0AL, UK.

²Bureau Veritas Consulting, 91-95 Winchester Road, Chandlers Ford, Hampshire, SO53 2GG, UK.

³Department of Mechanical Engineering, University College London, Torrington Place, London, WC1E 7JE, UK.

ABSTRACT

This paper presents an experimental and analytical study of crack shape evolution in steel specimens under cyclic loading. It is widely known that the introduction of compressive residual stresses by cold working the surface can be highly beneficial in improving the fatigue performance of structural components. Although it is recognised that relaxation of surface compressive residual stress can reduce the potential benefits, the effects of residual stress on crack shape evolution are often overlooked. A recently developed technique termed controlled stitch cold working, which applies differing intensities of compressive residual stress at specific regions in a structure, is shown in the paper to considerably influence fatigue crack propagation by containing crack propagation in one primary direction.

KEYWORDS

Residual Stress, Crack Shape Control, Fatigue, Surface Crack, Cold Rolling, RMS Stress Intensity Factors.

NOMENCLATURE

a	Crack Depth
c	Crack half-length
K	Stress Intensity Factor (SIF)
RMS	Root Mean Square
S	Crack Surface
T	Plate Thickness
Y	Normalised SIF or Y geometry correction factor
φ	Crack front angle

INTRODUCTION

The benefits of compressive residual stresses in enhancing fatigue performance are well known. Screw thread roots, shaft fillets and many other machine details are routinely cold rolled for this reason, and improvements in resistance to fatigue crack initiation by a factor of up to five fold are not uncommon [1 -3]. Features of residual stresses in metals are that they are often transient in nature and can relax under cyclic loading and at high temperature. The magnitude of residual stress a material can

contain is related to its yield strength, thus high strength materials can contain higher residual stresses and, in theory, can therefore benefit more from cold working treatment.

A previous paper [4] introduced the idea of controlling fatigue crack propagation through “stitch cold rolling”. The study was at the time in its infancy. This present paper reports further tests including one on a cracked specimen approaching 1×10^7 cycles, still exhibiting a slow linear crack growth rate. It also presents an analytical fracture mechanics approach that sets the basis for prediction of fatigue crack growth in anisotropic materials such as a surface cold worked component.

ANALYTICAL FRACTURE MECHANICS STUDY

Firstly, to briefly describe the context for the work, it should be appreciated that crack shape can be just as influential on crack propagation as applied load magnitude [5]. To illustrate this, Figure 1 below shows the well known Newman Raju flat plate surface crack Stress Intensity Factor (SIF) solution [6] around a crack front under tension, plotting Normalised SIF (or Y Factor) against crack angle ($0 \rightarrow \pi$) for a range of crack shapes (crack aspect ratio).

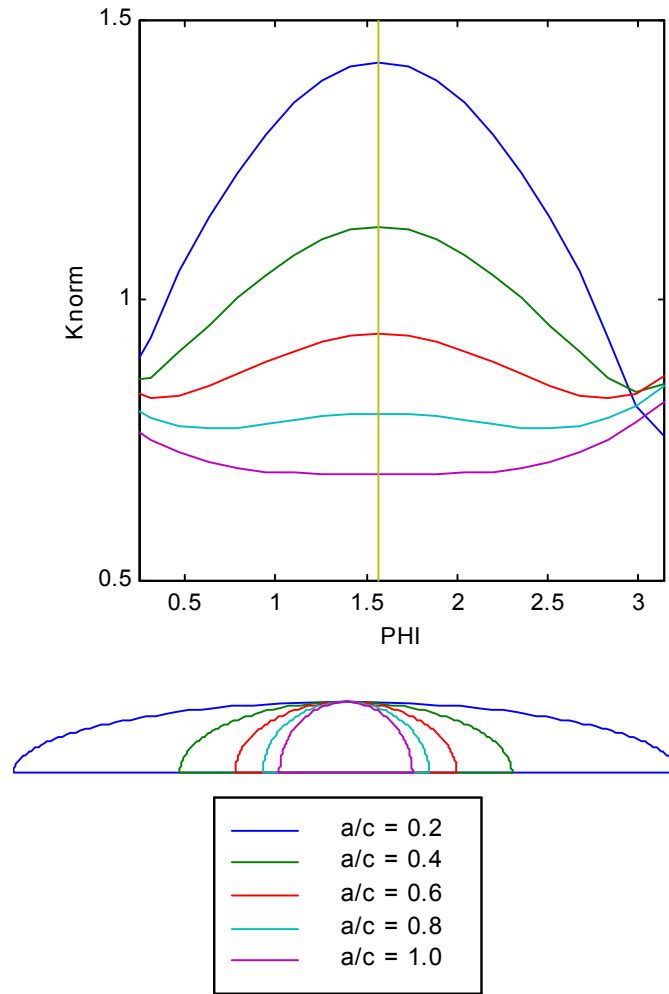


Figure 1. Newman Raju SIF Solutions [6] for different Shaped Cracks

At the crack deepest point ($\phi/2$) a very long crack with an aspect ratio of $a/c = 0.2$ has a high SIF compared with the value at the surface point. This crack therefore tends to grow faster at the deepest point meaning the crack aspect ratio becomes higher as the crack grows. A shorter crack of the same depth, say $a/c = 0.6$ has a far lower SIF at its deepest point, but still this is higher than the SIF at the surface. Taking the other extreme, a semi-circular crack ($a/c = 1.0$) has a higher SIF at the surface than at its

deepest point meaning it extends faster at the surface under cyclic fatigue loading resulting in a semi-ellipse with a lower aspect ratio. These observations are important for the predication of crack propagation behaviour but also suggest that if a crack shape can be prescribed or crack growth restricted in one direction, then the crack growth rate can be controlled.

A powerful method for describing the *SIF* around a crack front is the RMS SIF [7] approach. This considers crack growth in two principal directions: 1) in crack length (*c-direction*), and 2) in crack depth (*a-direction*). The *RMS* or average value for *SIF*, K_{rms} , enclosed by the area, S , can be derived from K_{rmsc} in the *c-direction* and K_{rmsa} in the *a-direction* (See Figure 2).

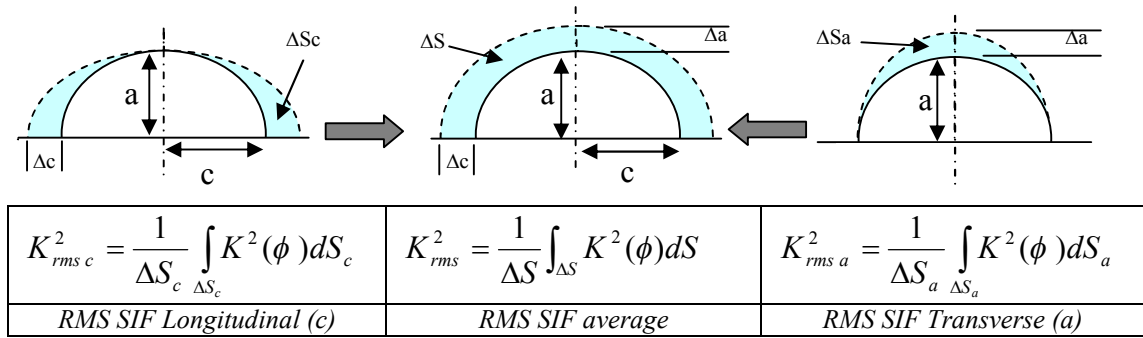
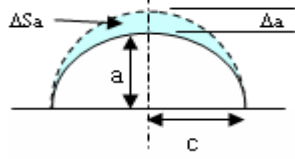
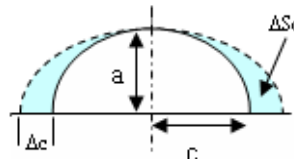
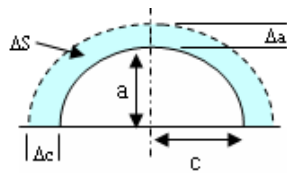


Figure 2. RMS Stress Intensity Factor

Derivation of the two independent *RMS SIFs* (K_{rmsa} and K_{rmsc}) with respect to the changes in shaded areas, ΔS , in *a-direction* (ΔS_a) and *c-direction* (ΔS_c) is shown below:

For the crack depth, or a-direction:	For the crack length or c-direction:
	
$K_{rms\ a}^2 = \frac{1}{\Delta S_a} \int_{\Delta S_a} K^2(\phi) dS_a \quad (1)$	$K_{rms\ c}^2 = \frac{1}{\Delta S_c} \int_{\Delta S_c} K^2(\phi) dS_c \quad (6)$
From Cruse and Besuner [7]:	From Cruse and Besuner [7]:
$\Delta S_a = \frac{1}{2} \pi c \Delta a \quad (2)$	$\Delta S_c = \frac{1}{2} \pi a \Delta c \quad (7)$
$dS_a = c \Delta a \sin^2 \phi d\phi \quad (3)$	$dS_c = a \Delta c \cos^2 \phi d\phi \quad (8)$
Substitute (2) and (3) into Eqn (1):	Substitute (7) and (8) into Eqn (6):
$K_{rms\ a}^2 = \frac{2}{\pi c \Delta a} \int_{\Delta S_a} [K(\phi)]^2 \times \Delta a c \sin^2 \phi d\phi \quad (4)$	$K_{rms\ c}^2 = \frac{2}{\pi a \Delta c} \int_{\Delta S_c} [K(\phi)]^2 \times \Delta c a \cos^2 \phi d\phi \quad (9)$
Hence:	Hence:
$K_{rms\ a}^2 = \frac{2}{\pi} \int_0^\pi [K(\phi)]^2 \times \sin^2 \phi d\phi$ $K_{rms\ a} = \sqrt{\frac{2}{\pi} \int_0^\pi [K(\phi)]^2 \times \sin^2 \phi d\phi} \quad (5)$	$K_{rms\ c}^2 = \frac{2}{\pi} \int_0^\pi [K(\phi)]^2 \times \cos^2 \phi d\phi$ $K_{rms\ c} = \sqrt{\frac{2}{\pi} \int_0^\pi [K(\phi)]^2 \times \cos^2 \phi d\phi} \quad (10)$
RMS SIF, $K_{rms\ a}$, for the depth direction.	RMS SIF, $K_{rms\ c}$, for the length direction.

Evaluating $K_{rms\ a}$ and $K_{rms\ c}$ in both directions, K_{rms} , Eqn. (11), as an average SIF for the entire crack front can be determined:



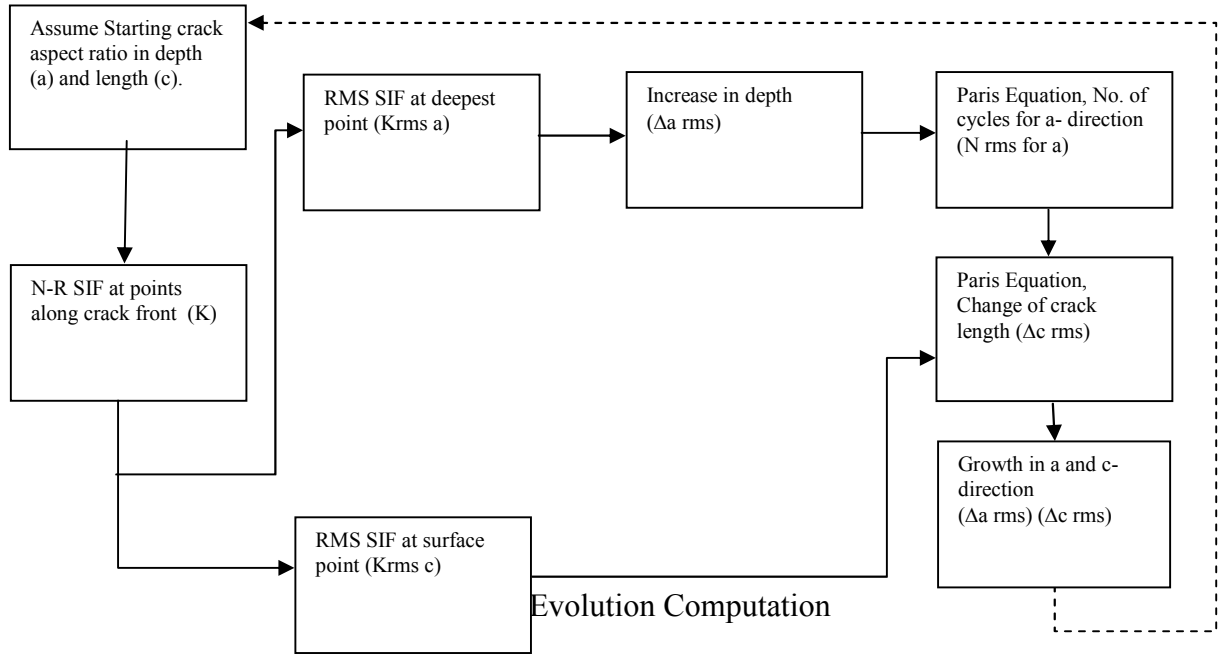
$$K_{rms}^2 = \frac{1}{\Delta S} \int_{\Delta S} K^2(\phi) dS \quad (11)$$

The Newman and Raju surface crack plate SIF solutions [6] can now be substituted and crack growth rates for the two directions calculated using the Paris Equation as follows:

For crack depth:
$$\frac{da_{rms}}{dN_{rms}} = C \Delta (K_{rms a})^m \quad (12)$$

For crack length:
$$\frac{dc_{rms}}{dN_{rms}} = C \Delta (K_{rms c})^m \quad (13)$$

A schematic of the crack growth evolution routine is shown in Figure 3:



The crack shape evolution computation shown above produces a crack propagation prediction in terms of an a - N and c - N curve and crack aspect ratio evolution. The program is designed to “loop” for increasing values of crack depth (a)

until it reaches half the plate thickness ($T/2$) with the corresponding change in crack length (c).

Figures 4 and 5 below show the prediction for a surface crack in a flat plat under tension and pure bending respectively. Many researchers have observed the behaviour illustrated by Figures 4 and 5 that irrespective of the initial or starting crack shape, the crack tends to an optimum aspect ratio for different types of structural components [8, 9]. This is independent of applied stress range assuming a single crack but can be affected by material anisotropy and certainly by loading mode (e.g. tension, bending, shear, etc.,).

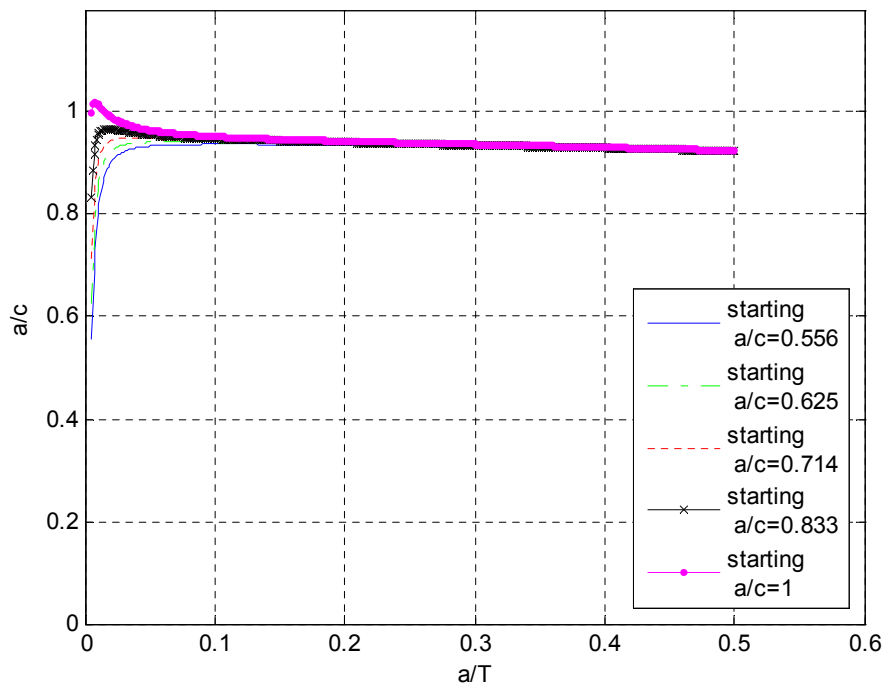


Figure 4. Predicted Crack Shape Evolution under tension.

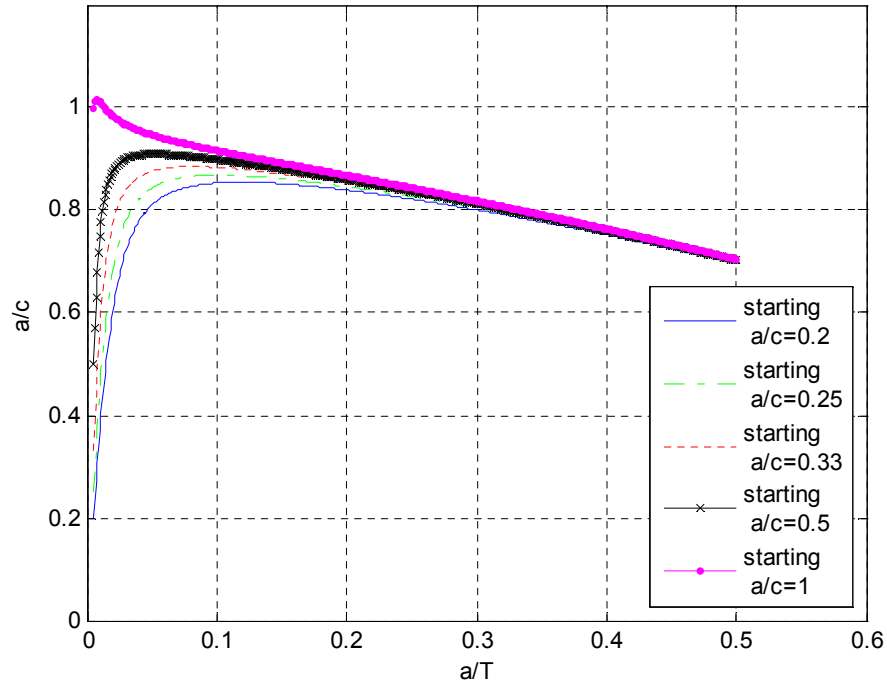


Figure 5. Predicted Crack Shape Evolution under bending.

EXPERIMENTAL TEST DETAILS

The test specimens were fabricated from BS EN 10025 Grade 275, a mild steel with a yield strength of 275MPa [10]. The plates were 790mm in length and 200mm in width; specimens 1 & 2 had a thickness of 40mm, specimens 3, 4 & 5 were 20mm thick.

Stitch rolling, where the central area of the plate was left unrolled, was performed using a purpose built cold rolling rig applying a force of 21kN to the roller placed in a machined notch on the plate surface and forced along the notch by a hydraulic jack.

Several rolling passes were applied, monitoring the applied load carefully during the rolling process. Table 1 details these and summarises the test parameters.

Table 1. Test Specimen Details.

Specimen	Plate	No. of Re-			
	Thickness (mm)	Cold Rolling Pressure (psi)	No. of Passes	roll Passes (after initiation)	Unrolled Length (mm)
Test 1	40	6000	3	3	20
Test 2	40	6000	3	3	40
Test 3	20	6000	4	0	20
Test 4	20	6000	5	0	20
Test 5	20	6000	5	0	40

Tests 1 and 2 were also rolled again following crack initiation as these were the first tests completed and it was unknown whether the residual stresses due to rolling would have remained during such a relatively large number of fatigue cycles. Tests 1, 3 and 4 had an unrolled length of 20mm, whereas tests 2 and 4 had a longer 40mm unprotected length. Table 2 summarises the fatigue test parameters and duration.

Table 2. Summary of Fatigue Tests.

Specimen	Nominal	Fatigue	No. of	
	Stress	Cycling	Cycles to	Total Test
	Range	Frequency	Crack	Cycles
	(MPa)	(Hz)	Initiation	
Test 1	122	4	128,000	4,000,000
Test 2	122	4	100,000	4,850,000
Test 3	120	4	345,000	3,718,000
Test 4	120	4	1,161,000	9,380,000
Test 5	120	4	500,000	6,000,000

Crack sizing and monitoring was by Alternating Current Potential Difference (ACPD) that allowed the depth and length of the cracks to be monitored in a non-destructive manner during testing. Figure 6 shows the type of data obtained; this allowed minimal interruption of fatigue cycling so that a large number of fatigue cycles could be applied.

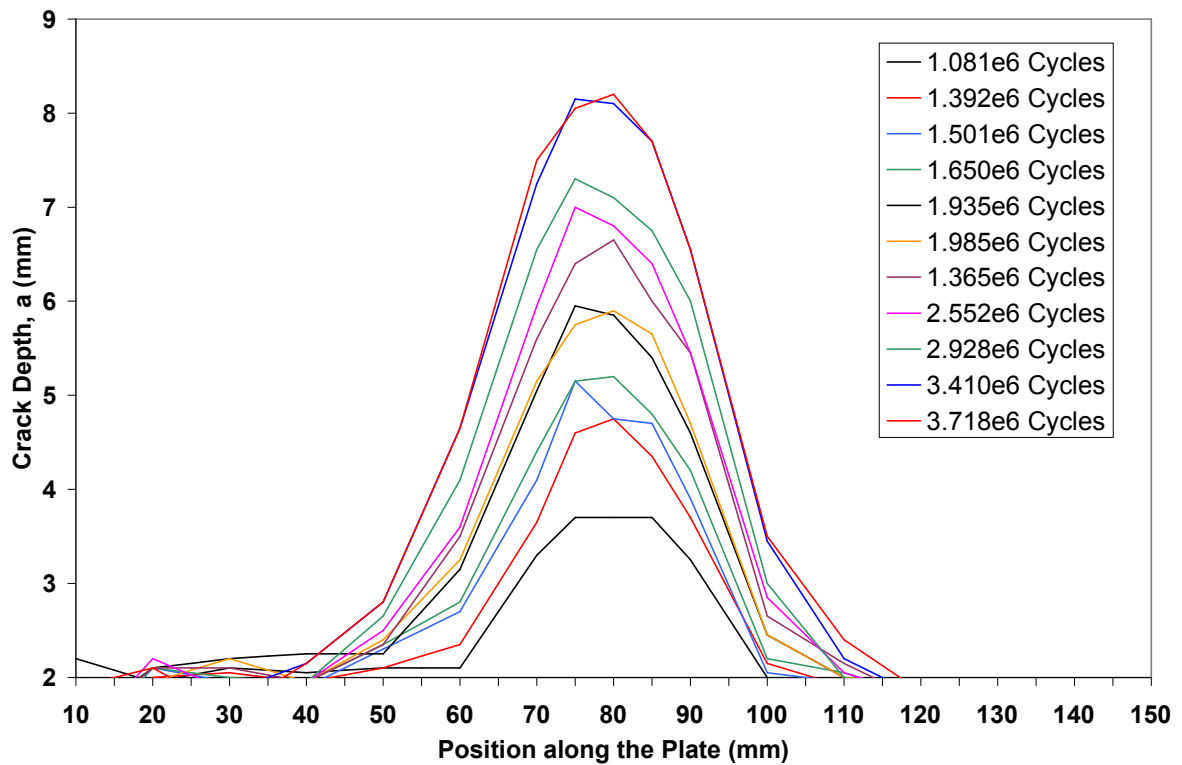


Figure 6. Crack Shape Evolution for Test 3.

FATIGUE TEST RESULTS

Figure 7 below shows the fatigue crack growth results for all the tests. None of the cracks grew through the plate thickness or width, and tests were terminated due to cracks initiating at other locations (at the specimen edges) or for reasons of time and project resources.

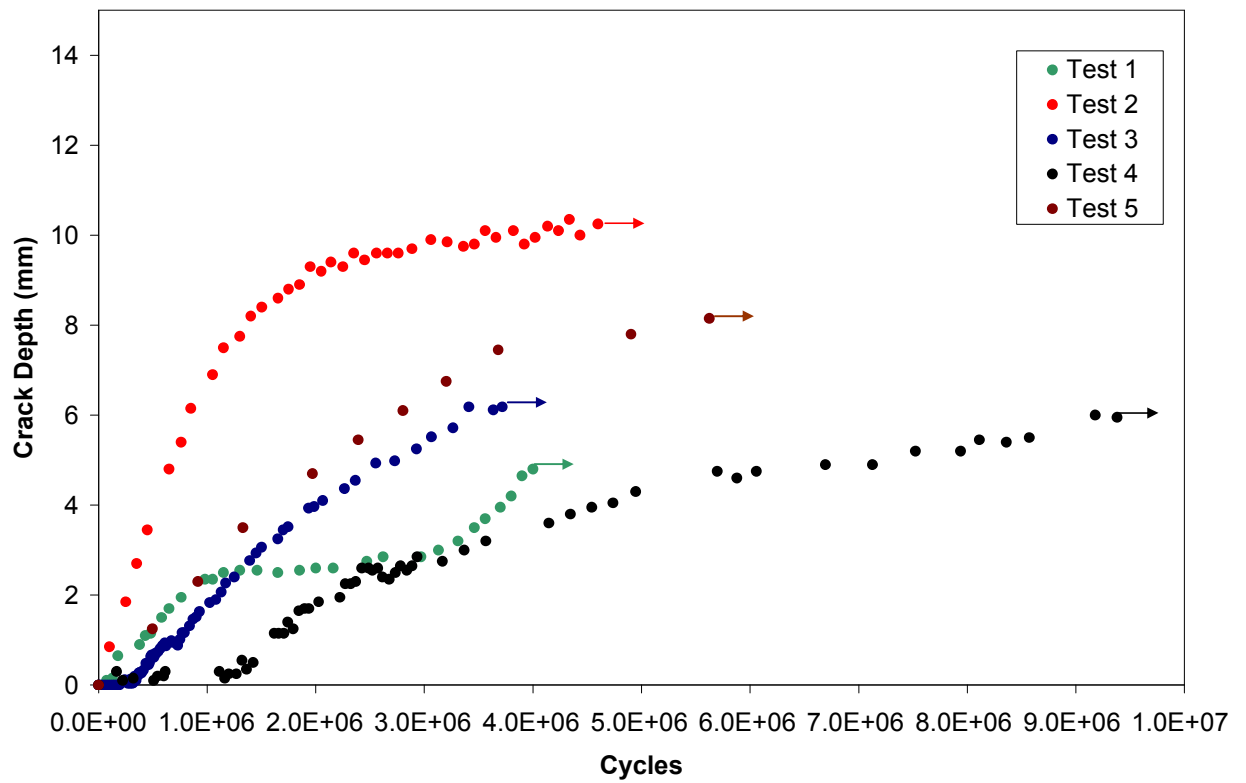


Figure 7. Crack Growth Data for all Tests.

Following testing, specimens were cooled in liquid nitrogen and broken open to observe the fatigue crack surface. Figure 8 below firstly shows a typical crack shape (beachmarked to highlight the shape evolution) from an artificial starter notch growing in a semi-elliptical manner. This is contrasted by the crack shape observed from Tests 1 and 2 and to a lesser degree tests 4 and 5. Beach marks on the surfaces of Tests 4 and 5 show similar unusual crack shapes to specimens 1 and 2.

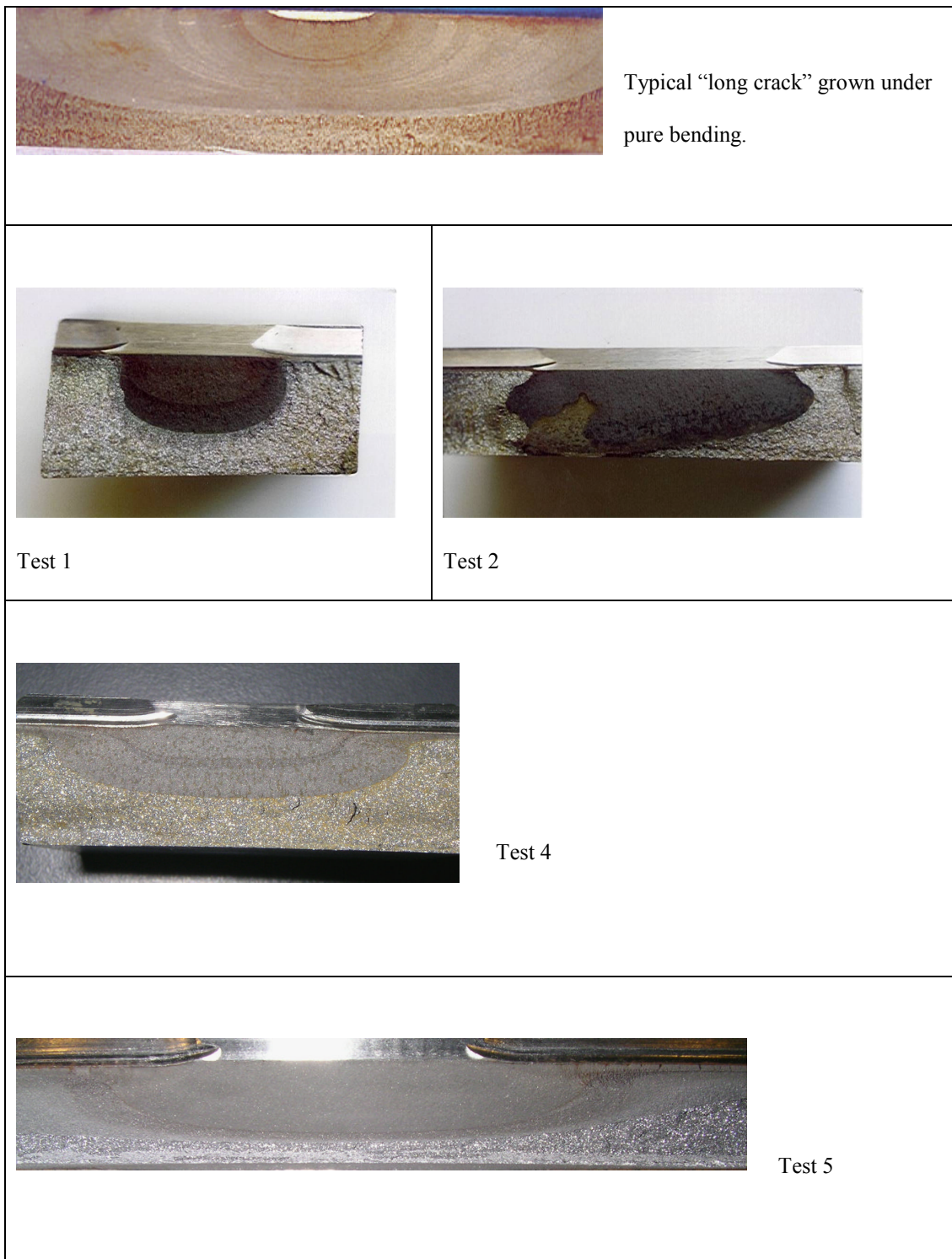


Figure 8. Fracture Surfaces.

DISCUSSION

The crack growth data in Figure 7 are clearly unusual not only due to the very slow crack propagation rates, but also several tests clearly show a retardation effect. All tests show normal fatigue crack growth until the crack extends out of the unrolled length to meet with the cold rolled region. Tests 2 & 5 had the longest unrolled length (40mm) and the results clearly show deeper cracks despite these having two different values of plate thickness. Neither test showed a clear resumption of growth following arrest but again it should be noted the tests were terminated prematurely. Test 3 showed similar behaviour, Tests 1 and 4 clearly show recovery following retardation. These tests differed in the plate thicknesses but also that Test 1 was rerolled after crack initiation. Test 4 shows the extraordinary propagation life of greater than 8×10^6 cycles, a comparative unrolled propagation life would be in the order of 1.5×10^6 cycles using a Newman Raju based prediction.

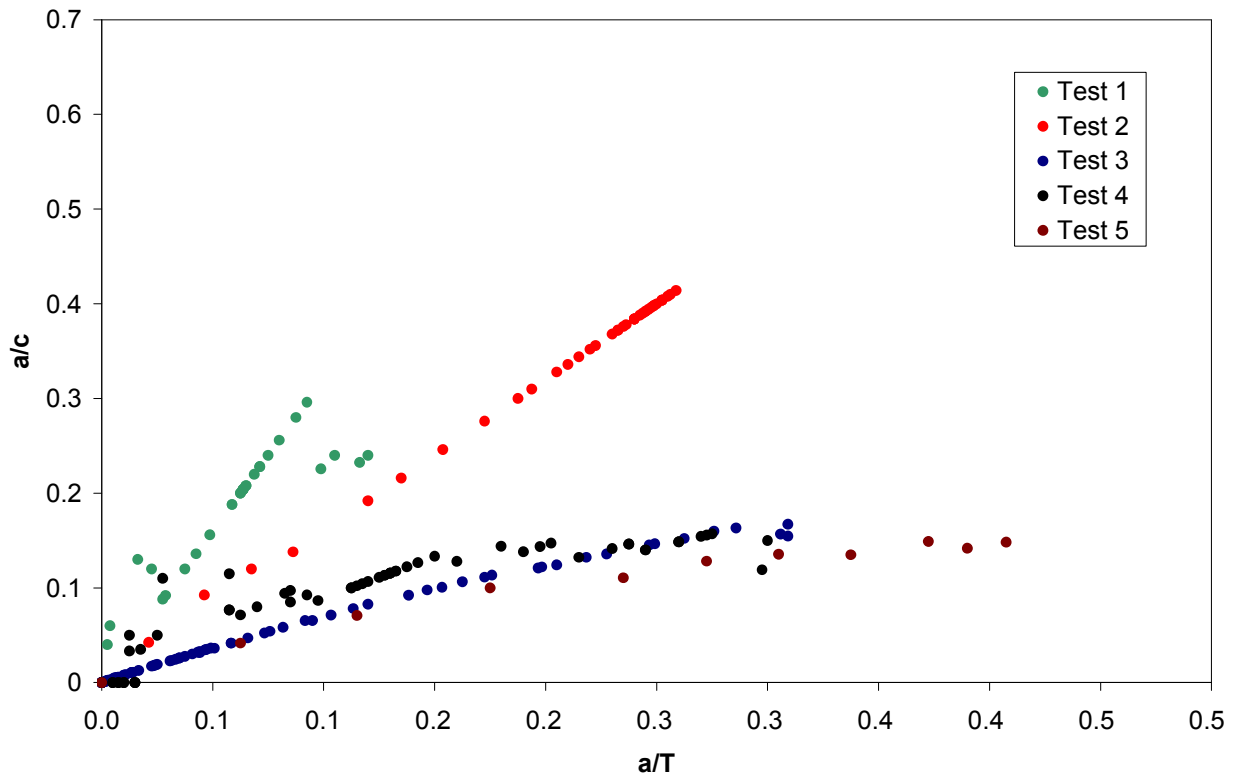


Figure 9. Crack Shape Evolution Data for all Tests.

Figure 9 shows the crack aspect ratio data. If this is compared with Figure 5, it is appreciated that the crack shapes have in all cases been altered significantly from their optimum aspect ratio. Under bending these cracks have higher stress at the surface point as they grow towards the neutral axis. It appears clear for the relatively thin plates tested that under pure bending, it is unlikely that a crack could be encouraged to grow to through thickness. This would not be the case under axial tension, and at this point, it is

hypothesised that axial tension should produce a leak-before-break crack. The retardation and, in some cases, the crack arrest effect however is remarkable.

CONCLUSIONS AND FUTURE WORK

The following conclusions can be drawn:

- An RMS SIF approach can be used to predict crack growth evolution. In this paper, has not been compared with the experimental results, as the solution does not currently model the cold rolling residual stress effects.
- Controlled surface cold working can significantly retard fatigue crack propagation.
- The effects of cold working were observed for several million cycles at a nominal cyclic stress close to half yield stress.
- Cracks loaded under bending extended only very slowly in depth when the length was contained by cold working meaning that through thickness cracks are unlikely.

Current work at Cranfield University involves axial tests on shot peened and laser peened specimens. In addition, residual stress measurements are being made and in

parallel the analytical fracture mechanics model is under development to use SIF weight functions [11] to incorporate residual stress effects. It is anticipated that experience with fatigue testing and development of analytical tools will allow the use of stitch/preferential cold working in structural components to extend life and develop the concept of controlled failure design.

ACKNOWLEDGEMENTS

The authors gratefully acknowledge the financial support of NDE Technology Limited in funding this work, Lt J Boyle (RN) for carrying out Test 3, and Ms S Ng for Tests 4 & 5.

REFERENCES

1. Knight, M. J., Brennan, F. P. and Dover, W. D., (2003) *Fatigue Fract Engng Mater Struct* **26**, 1081–1090.
2. Knight, M. J., Brennan, F. P. and Dover, W. D., (2004) *NDT and E International*, **37**, No 5, 337-343.
3. Knight, M. J., Brennan, F. P. and Dover, W. D., (2005) *The Journal of Strain Analysis for Engineering Design*, **40**, No. 2, 83-93.

4. Ngiam, S.S. and Brennan, F. P., (2003), *International Conference on Fatigue Crack Paths*.
5. Brennan, F. P., (1997) in *Proceedings of the 13th international Ship and Offshore Structures Congress*, **3**, Editors Moan, T. and Berge.
6. Newman, J.C. and Raju, I.S., (1981) *Engineering Fracture Mechanics* **15**, 185-192.
7. Cruse, T. A. and Besuner, P. M., (1975) *Journal of Aircraft*, **12**, **No. 4**, 369-375.
8. Carpinteri, A. (1993) *Int. J. Fatigue*, **15**, **No. 1**, 21-26.
9. Carpinteri, A., Brighenti, R., Spagnoli, A. (2000) *Int. J. Fatigue*, **22**, **No. 1**, 1-9.
10. BS EN 10025:2004 *The British Standard Institute*.
11. Brennan, F. P. and Teh, L.S., (2004) *Fatigue Fract Engng Mater Struct* **27**, 1–7.